

Abnormal grain growth and liquid-phase sintering in $\text{Sr}_{0.6}\text{Ba}_{0.4}\text{Nb}_2\text{O}_6$ (SBN40) ceramics

HAN-YOUNG LEE*, R. FREER†

Materials Science Centre, University of Manchester/UMIST, Grosvenor Street, Manchester M1 7HS, UK

E-mail: Robert.Freer@umist.ac.uk.

Ceramics of $\text{Sr}_{0.6}\text{Ba}_{0.4}\text{Nb}_2\text{O}_6$ (SBN40) were prepared by the conventional mixed oxide route. Sintering at temperatures $\geq 1260^\circ\text{C}$ led to rapid, non-uniform grain growth and a duplex microstructure. Presintering at 1250°C followed by higher temperature sintering ($1350\text{--}1450^\circ\text{C}$) controlled grain growth. Rapid cooling from 1450°C froze-in second phases at grain boundaries. Scanning electron microscopy and transmission electron microscopy showed that the resulting grain-boundary phases were Nb_2O_5 -rich and BaO-deficient, having low liquid-formation temperatures. In contrast, SBN40 ceramics prepared with excess BaO and a deficiency of Nb_2O_5 showed no enhancement of grain growth at the highest temperature. Sintering behaviour and microstructural development provide evidence for the existence of a liquid phase which assists abnormal grain growth. The effect of presintering in controlling grain growth is discussed, and a mechanism for abnormal grain growth in $\text{Sr}_{0.6}\text{Ba}_{0.4}\text{Nb}_2\text{O}_6$ (SBN40) ceramics is proposed. © 1998 Chapman & Hall

1. Introduction

Strontium barium niobate ($\text{Sr}_{1-x}\text{Ba}_x\text{Nb}_2\text{O}_6$, SBN) has a tetragonal, tungsten bronze (TTB) structure with --Nb--O--Nb--O-- polar chains which give rise to a network of NbO_6 octahedra. The TTB phase in SBN, where only five A-sites are occupied out of six, can be obtained in a wide range of compositions ($0.25 \leq x \leq 0.75$) and even in cation-excess, non-stoichiometric solid solutions [1]. This allows the fabrication of materials having a wide range of compositions, appropriate for different applications. The physical and dielectric properties are critically dependent on the Sr/Ba ratio, which determines the structural entropy [2] and the distribution of strontium and barium cations and vacancies [3]. From the structural point of view, there is a common feature between TTB and perovskite structures in that both are based on a network of oxygen octahedra. The TTB structure can be transformed to the perovskite structure by a 45° rotation of four oxygen octahedra surrounding the A_1 -site, which makes one TTB unit $[(A_1)_2(A_2)_4(C)_4(B_1)_2(B_2)_8O_{30}]$ equivalent to ten perovskite units $[ABO_3]$ [4].

In recent years, a number of alkali and alkaline-earth niobates have been investigated for applications in electro-optics (utilizing their large electro-optic effects or large non-linear optic effects [5, 6], as well as for applications in pyroelectric detectors and piezoelectric transducers [7, 8]). Strontium barium niobate is one of the most promising of these materials. Great

difficulty was encountered in the growth of single-crystal SBN and this led to interest in the fabrication of transparent SBN ceramics by means of compositional modification [9] and hot-pressing [10, 11]. Unfortunately, unusual sintering behaviour, in the form of rapid, abnormal grain growth, was found in SBN40 [12], SBN70 [13] and potassium strontium niobate (KSN) ceramics [14]. It is apparent that the dielectric properties (Curie temperature, relative permittivity, dielectric loss, the broadness of dielectric maxima and spontaneous polarization) of SBN ceramics are significantly affected by the microstructure [15–17].

We have reported that abnormal grain growth in SBN ceramics is caused by the presence of a liquid phase whose composition deviates from $[\text{Nb}_2\text{O}_5 : (\text{SrO} + \text{BaO}) = 1 : 1]$ and tentatively proposed a possible mechanism for abnormal grain growth [18]. This study examines abnormal grain growth in SBN40 ceramics and presents direct and indirect evidence for the existence and role of the grain-boundary phase in SBN ceramics. The benefits of presintering (to achieve compositional homogenization) and fast heating (to give uniform wetting of grains by the liquid phase) are also discussed.

2. Experimental procedure

Electronic grade powders (purity $> 99.5\%$) of strontium carbonate, barium carbonate and niobium

* Present address: Korea Electronics Technology Institute, #455-6 Masau-ri, Jinwi-myun, Pyungtaek-si, Kyunggi-do 4510860, Korea.

† Author to whom all correspondence should be addressed.

pentaoxide were used as starting materials. Four kinds of SBN40 ceramic specimens were prepared as follows:

1. SBN40cs: $\text{Sr}_{0.6}\text{Ba}_{0.4}\text{Nb}_2\text{O}_6$ ceramics conventionally sintered at 1250–1300 °C;
2. SBN40ds: $\text{Sr}_{0.6}\text{Ba}_{0.4}\text{Nb}_2\text{O}_6$ ceramics sintered at 1350–1400 °C following presintering at 1250 °C;
3. SBN40dsh: $\text{Sr}_{0.6}\text{Ba}_{0.4}\text{Nb}_2\text{O}_6$ ceramics sintered at 1450 °C with rapid heating and cooling ($\pm 600^\circ\text{C h}^{-1}$) following presintering at 1250 °C;
4. SBN40m: modified $\text{Sr}_{0.6}\text{Ba}_{0.4}\text{Nb}_2\text{O}_6$ ceramics (with 1.25 mol % excess BaO and 0.5 mol % deficient Nb_2O_5) conventionally sintered at 1400–1450 °C.

The powder mixtures in appropriate molar ratios were wet-milled with ethanol in a vibration-type mixer for 24 h using ZrO_2 balls as media. Dried powder mixtures were calcined at 1200 °C and then compacted in a die of 10 mm diameter under a uniaxial pressure of 100 MPa. The heating and cooling rates, except for SBN40dsh (as noted above), were $\pm 240^\circ\text{C/h}$. The holding time for calcination and sintering was 4 h. The sintered products were sliced into discs ~ 1 mm thick, ground and then polished using 6 and 1 μm diamond paste and finally 0.03 μm Al_2O_3 powder suspension in an automatic polishing machine (Buehler, UK). Surfaces of as-sintered or polished and thermally etched (at 1200 °C for 20 min) specimens were gold-coated prior to SEM analysis (Philips model 505 and 525). Transmission electron microscopy (TEM) specimens were prepared by mechanically polishing 3 mm diameter discs down to 20–30 μm thickness using a dimpler (VCR, USA) and ion-beam thinning (Iontech, UK) at 2 mA and 5 kV to achieve electron transparency. A Philips TEM, model EM430, was used to investigate the specimens.

3. Results and discussion

The microstructures of SBN40 ceramics prepared by conventional and dual-stage sintering have been described in detail elsewhere [18]. For the sake of completeness and to aid discussion of mechanisms, examples are reproduced here.

3.1. Conventional sintering behaviour

The microstructures of SBN40 ceramics (specimens SBN40cs) sintered at different temperatures, 1250, 1260 and 1300 °C are shown in Fig. 1. It can be seen that abnormal grain growth commences at a specific temperature ($\sim 1260^\circ\text{C}$) in a localized area of the specimen (Fig. 1b). The process becomes active by a small increase of sintering temperature and leads to the development of a duplex structure comprising very large (up to 1 mm) grains and relatively small “pillar-type” grains (Fig. 1c). This implies the existence of a liquid phase with liquid-formation temperature lower than that of the required sintering temperature, and that abnormal grain growth occurs in limited areas around the molten phases at the sintering temperatures. Pejovnik *et al.* [19] found that during liquid-phase sintering of alumina, the major portion of densification occurred within the first 10 min after

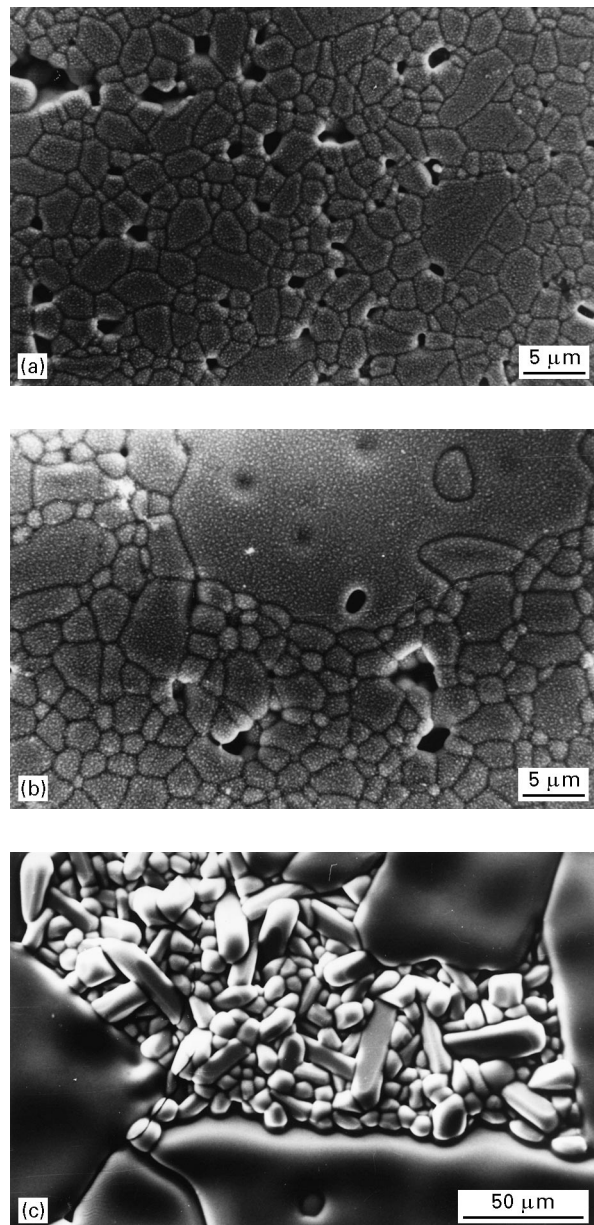


Figure 1 Scanning electron micrographs of SBN40 ceramics sintered at (a) 1250, (b) 1260 and (c) 1300 °C.

melt formation. This is consistent with the experimental results of Kimura *et al.* [14] which demonstrated that sintering KSN at 1350 °C for 10 min led to the formation of extremely large grains. Because Kimura *et al.* employed a low heating rate (100°C h^{-1}) it is probable that a liquid phase might have formed at a much lower temperature, although the possibility of liquid-phase sintering giving rise to abnormal grain growth was not considered in any detail in their work.

3.2. Dual-stage sintering behaviour

After low-temperature sintering at 1250 °C (presintering), some specimens were sintered at higher temperatures (dual-stage sintering). SEM microstructures of SBN40 ceramics dual-stage sintered (specimens SBN40ds) at 1350 and 1400 °C are shown in Fig. 2a and b. Inhibition of abnormal grain growth up to a

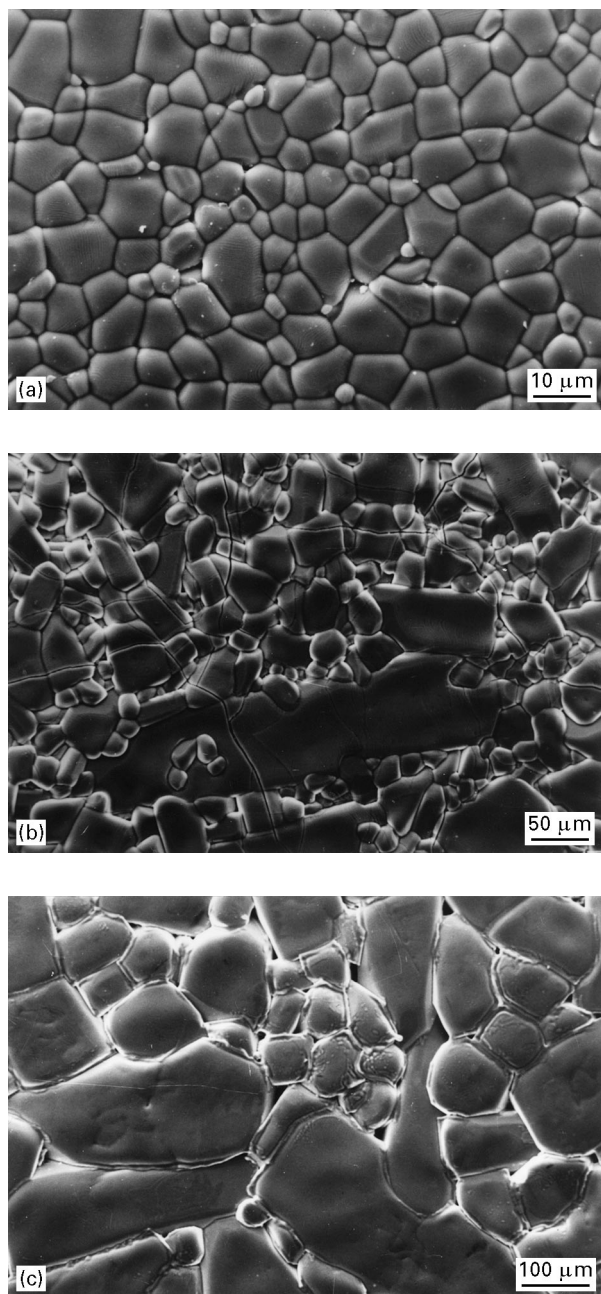


Figure 2 Scanning electron micrographs of SBN40 ceramics dual-stage sintered at (a) 1350 °C, (b) 1400 °C and (c) at 1450 °C. Heating and cooling rates were $\pm 240\text{ °C h}^{-1}$ for (a) and (b), $\pm 600\text{ °C h}^{-1}$ for (c).

particular temperature, i.e. at least 1350 °C, after presintering indicates the transformation of liquid phase to the primary phase (i.e. the starting composition). The microstructures of as-fired surfaces of SBN ceramics (specimens SBN40dsh) dual-stage sintered at high temperatures (1450 °C) with rapid heating and cooling rates ($\pm 600\text{ °C h}^{-1}$) clearly show a substantial grain-boundary phase in every grain boundary (Fig. 2c). The primary grains are well separated and coated by the grain-boundary phase. It appears that there was a large amount of liquid phase which wet all the grains, enabling them to grow abnormally large.

3.3. Transmission electron microscopy

In contrast to the uniformly large grains in the as-fired surfaces of SBN40dsh sintered at 1450 °C, polished

and etched surfaces exhibited slightly smaller grains with less well developed grain-boundary phases. In the interior of the specimens, many of the grains possessed clean grain boundaries and there were comparatively few grain-boundary phases although preferential milling of the grain boundaries may have occurred during ion-beam thinning.

TEM analysis of SBN40dsh specimens revealed compositional differences between the grains and grain boundaries (Fig. 3). The grain-boundary phases were Nb_2O_5 -rich and BaO-deficient. For the primary grains $[\text{Sr}/\text{Ba}] = 1.46$ and $[\text{Nb}_2\text{O}_5/(\text{SrO} + \text{BaO})] = 0.98$; for the grain boundaries $[\text{Sr}/\text{Ba}] = 3.08$ and $[\text{Nb}_2\text{O}_5/(\text{SrO} + \text{BaO})] = 1.55$. There was evidence of variability in the composition of the grain-boundary phase from one grain to another, i.e. the liquid phase was not homogeneous in composition. A phase diagram [1] of the ternary system SrO–BaO– Nb_2O_5 indicates that the Nb_2O_5 -rich compositions have low liquid formation temperatures, e.g. 1300 °C for SBN30 and 1312 °C for SBN40. Therefore, the second phases in the specimens with $[\text{Nb}_2\text{O}_5/(\text{SrO} + \text{BaO})] > 1$ should have reacted as liquid phases by melting at temperatures lower than the sintering temperature. The liquid phase contributes to rapid grain growth during sintering, whilst at the same time its own composition is adjusted towards that of the matrix phase (due to dissolution of the primary phase). Therefore, SBN ceramics with a duplex structure (Fig. 2b) show no compositional differences between the abnormally large grains and grains of “normal” size. Only rapid cooling from high temperature freezes the liquid phase in the grain boundaries before the compositional transformation is completed (Figs 2c, 3a and b).

Moiré patterns were observed in a number of ion-beam-thinned TEM specimens. Such patterns probably result from either (i) the presence of a thin, film-like phase, having a structure different from that of TTB, or different orientation, which covers the primary grains, or (ii) that the thin phase is of TTB structure, but mismatched in lattice alignment, resulting in a superimposed lattice image. Neither possibility can be excluded at this stage.

3.4. Sintering behaviour of modified SBN40 ceramics

The microstructure of the as-fired surface of an SBN40 ceramic (conventionally sintered at 1450 °C, specimen SBN40m) with 1.25 mol % excess BaO and 0.5 mol % deficient Nb_2O_5 is shown in Fig. 4. Most grains have nodular shape, similar to that of pillar-type grains found in SBN ceramics having a duplex structure. Unlike the stoichiometric compositions, no abnormal grain growth was observed after sintering at temperatures as high as 1450 °C. Although agglomerated grains were widely distributed, they did not develop into unusually large grains. In fact, the grain-growth rate was so slow that the average grain size was $\sim 7\text{--}8\text{ }\mu\text{m}$ and many pores remained unfilled. In spite of the high-temperature sintering, the resulting density ($\sim 95\%$ theoretical value) was not high, compared

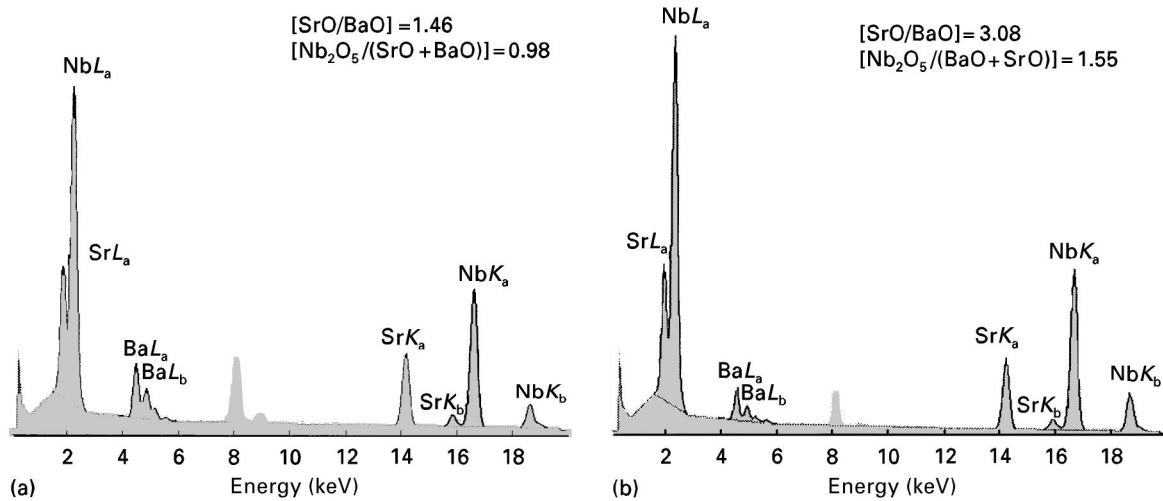


Figure 3 TEM EDS spectra for SBN40 ceramics dual-sintered at 1450 °C and with fast heating and cooling rates ($\pm 600^\circ\text{C h}^{-1}$) after presintering at 1250 °C; (a) the primary phase and (b) the grain boundary phase (only lanthanum peaks were used for analysis).

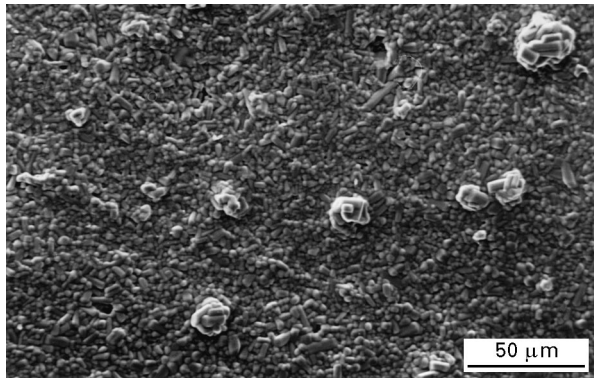


Figure 4 Scanning electron micrograph of as-sintered surface of SBN40 ceramic prepared with 1.25 mol % excess BaO and 0.5 mol % deficient in Nb_2O_5 .

TABLE I Evidence for the existence of liquid phase which results in the formation of a second phase in SBN ceramics

| | |
|--|--|
| Sintering behaviour | Narrow range of sintering temperatures for abnormal grain growth |
| SEM microstructures | Continuous grain-boundary phase coating the primary grains |
| TEM microstructures | Direct imaging of grain-boundary phase; preferential etching during ion-beam thinning |
| EDS analysis | Second phase with composition different from that of the matrix |
| Moiré patterns | Showing the presence of a phase with a structure different from that of the matrix |
| BaO-excess and Nb_2O_5 -deficient SBN ceramics | No abnormal grain growth up to 1450 °C; small size of resulting grains ($\sim 7\text{--}8\ \mu\text{m}$ on average) |

with that of SBN40dsh ceramics ($\sim 98.5\%$ theoretical density) sintered at the same temperature.

The contrasting behaviour of the stoichiometric and modified SBN40 suggest that without the presence of the Nb_2O_5 -rich and BaO-deficient phase, enhanced grain growth in SBN ceramics is minimal. Clearly grain growth in SBN ceramics depends upon the starting composition of the powder and sintering temperature, but is sensitive to local compositional differences, particularly in the amounts of BaO and Nb_2O_5 .

3.5. The mechanism of abnormal grain growth in SBN ceramics

Several types of evidence to support the idea of liquid-phase sintering in SBN ceramics have been presented in this work. They are summarized in Table I. SEM and TEM microstructures, including Moiré patterns in the specimens sintered at high temperatures with rapid heating rates, revealed the existence of grain-boundary phases. It was found by chemical analysis (EDS) that such phases were rich in Nb_2O_5 and deficient in BaO, compared with the starting composition.

This led to the development of grain-boundary phases with lower liquid-formation temperatures. The sintering behaviour of modified SBN40 ceramics (with excess BaO and deficient Nb_2O_5 in the starting powders) supports the hypothesis that abnormal grain growth in SBN ceramics was caused by the liquid phase which was rich in Nb_2O_5 and deficient in BaO.

The mechanism of abnormal grain growth and the effect of presintering in SBN40 ceramics were discussed in detail in an earlier study [18]. The main stages are shown schematically in Fig. 5 and can be summarized as follows. The wide compositional range of SBN solid solubility in the system SrO–BaO– Nb_2O_5 and partially uncompleted calcination allows the formation of phases rich in Nb_2O_5 and deficient in BaO in localized areas (Fig. 5a(i)). These phases have liquid-formation temperatures lower than the normal firing temperature required for high density, and the liquid-formation temperature varies according to composition; the higher the deviation of the composition from $[\text{Nb}_2\text{O}_5 : (\text{SrO} + \text{BaO}) = 1:1]$, the lower the liquid-formation temperature. Unlike “normal” liquid-phase sintering, grain growth in SBN ceramics

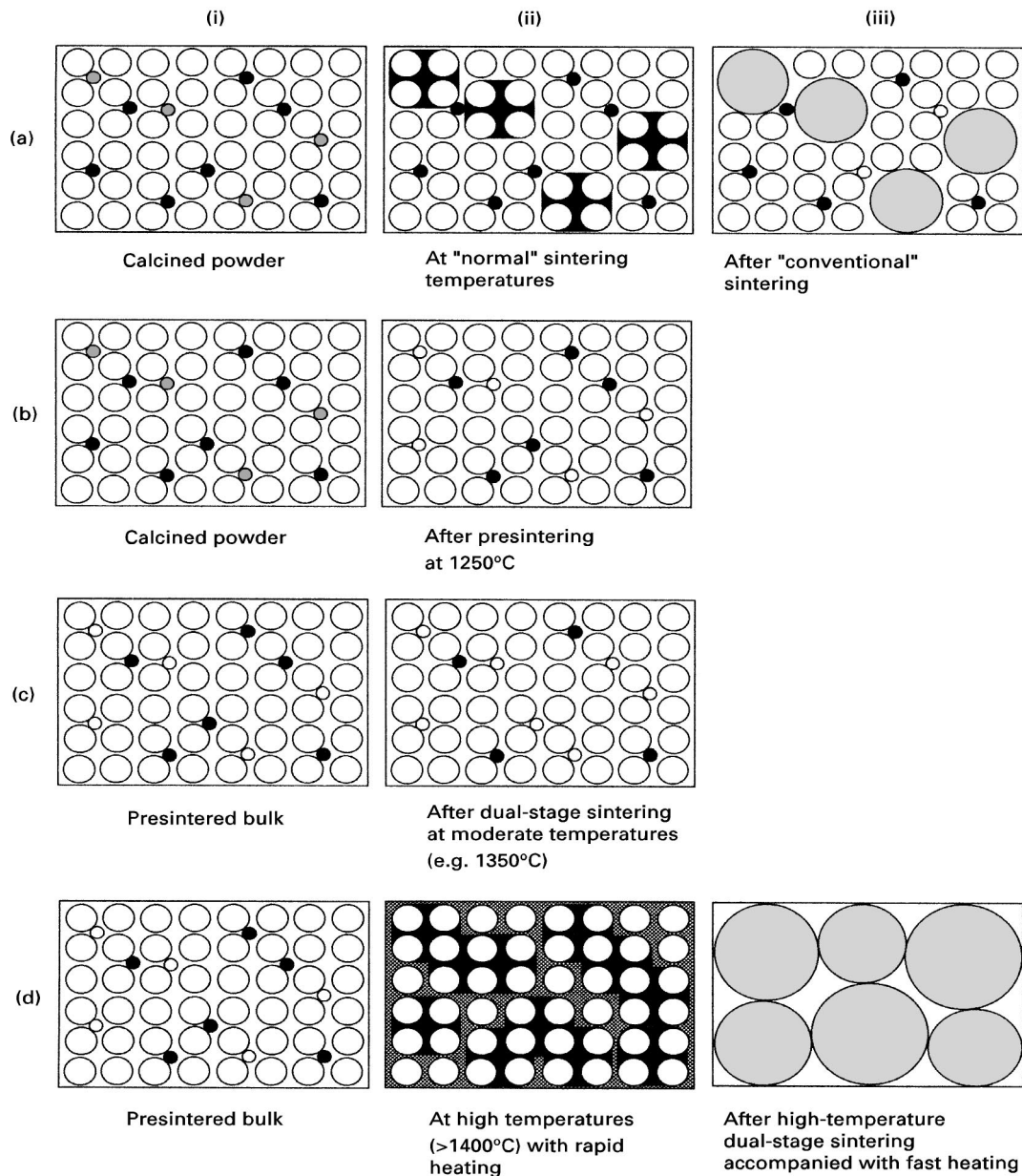


Figure 5 Schematic diagrams for sintering processes in SBN40 ceramics: (a) the “normal” process leading to abnormal grain growth; (b) presintering, (c) inhibition of abnormal grain growth by dual-stage sintering; (d) rapid heating at high temperatures after presintering. Shaded circles represent localized grain-boundary phases, having different liquid-formation temperatures. (○) Phases transformed to compositions close to $[\text{Nb}_2\text{O}_5 : (\text{SrO} + \text{BaO}) = 1:1]$, (■) liquid phases, (○) large grains grown by the liquid-phases mechanism.

appears to be localized before the liquid phases spread out through all the grains (Fig. 5a(ii)). Growth of the primary grains is rapid (Fig. 5a(iii)) because of the presence of the liquid phase; reactions between the two phases tend to adjust the composition of the liquid phase towards that of the initial composition of the powder. It is reasonable to expect some solubility of the solid phase in the liquid phase because of compositional similarity between the solid and liquid phases. The solid phase dissolved in the liquid phase will adjust the composition of the liquid phase towards $[\text{Nb}_2\text{O}_5 : (\text{SrO} + \text{BaO}) = 1:1]$. Compositional change of the liquid phase will cease when the liquid-formation temperature exceeds the sintering temperature. At that point, the interfacial energy between solid and liquid phases will be minimized and the liquid phase will solidify. Thus, at a given temperature, liquid-phase sintering will tend to occur at selected

parts of a specimen and abnormal grain growth will be localized. Presintering at temperatures below the onset temperature of abnormal grain growth enables a liquid phase, with liquid-formation temperature near to the presintering temperature, to react with and be transformed to a composition nearer to $[\text{Nb}_2\text{O}_5 : (\text{SrO} + \text{BaO}) = 1:1]$, as a form of compositional homogenization process (Fig. 5b). Thus, only grain-boundary phases (liquid phases) with higher liquid-formation temperatures remain after presintering (Fig. 5c(i)), and this enables subsequent high-temperature sintering without abnormal grain growth (Fig. 5c(ii)). Sintering at high temperature with a rapid heating rate leads to the generation of high-mobility liquid phases which encourage a uniform microstructure (Fig. 5d(ii)). The use of high-temperature, dual-stage sintering with a rapid heating rate gives large, uniform grains (Fig. 5d(iii)).

4. Conclusion

Microstructural and compositional evidence to support a model for unusual microstructure development in SBN40 ceramics has been presented. The sintering behaviour (abnormal grain growth in localized areas, commencing at a critical temperature lower than the required sintering temperature) can be explained on the basis of liquid-phase sintering. SEM and TEM investigations of SBN40 cooled rapidly from 1450 °C showed grain-boundary phases; EDS analysis revealed that the phases were Nb₂O₅-rich and BaO-deficient. They acted as liquid phases due to low liquid-formation temperatures. The production of a liquid phase was believed to result from locally inhomogeneous compositions (Nb₂O₅/(SrO + BaO) > 1) which, in turn, resulted from a partially incomplete calcination process. Presintering effectively inhibited non-uniform grain growth by transforming the composition of the second phases (i.e. liquid phases) nearer to that of the starting composition; this enabled subsequent high-temperature sintering. Large grains were not formed in SBN40 ceramics prepared with excess BaO and a deficiency of Nb₂O₅. It is concluded that the unusual microstructure development in SBN40 ceramics is due to Nb₂O₅-rich and BaO-deficient phases, acting as liquid phases, and that compositional homogenization by presintering prevents such abnormal grain growth.

References

1. J. R. CARRUTHERS and M. GRASSO, *J. Electrochem. Soc. Solid State Sci.* **117** (1970) 1426.
2. A. M. GLASS, *J. Appl. Phys.* **40** (1969) 4699.

3. R. GUO, A. S. BHALLA, G. BURNS and F. H. DACOL, *Ferroelectrics* **93** (1989) 397.
4. A. M. VARAPRASAD, *Jpn J. Appl. Phys.* **24** (1985) 361.
5. G. A. RAKULIJIC, K. SAYANO, A. AGRANAT, A. YARIV and R. NEURGAONKAR, *Appl. Phys. Lett.* **53** (1988) 1465.
6. D. RYTZ, B. A. WECHSLER, R. N. SCHWARTZ and C. C. NELSON, *J. Appl. Phys.* **66** (1989) 1920.
7. Y. H. XU, Y. YUAN, Y. YU and K. B. XU, *Proc. SPIE* **1220** (1990) 64.
8. P. M. XU and A. VAN DER ZIEL, *Ferroelectrics* **45** (1982) 247.
9. S. I. LEE and W. K. CHOO, *ibid.* **87** (1988) 209.
10. K. NAGATA, Y. YAMAMOTO, H. IGARASHI and K. OKAZAKI, *ibid.* **38** (1981) 853.
11. N. S. VANDAMME, A. E. SUTHERLAND, L. JONES, K. BRIDGER and S. R. WINZER, *J. Amer. Ceram. Soc.* **74** (1991) 1785.
12. J. TAKAHASHI, S. NISHIWAKI and K. KODAIRA, *Ceram. Trans.* **41** (1994) 363.
13. S. NISHIWAKI, J. TAKAHASHI and K. KODAIRA, *Jpn J. Appl. Phys.* **33** (1994) 5477.
14. T. KIMURA, S. MIYAMOTO and T. YAMAGUCHI, *J. Amer. Ceram. Soc.* **73** (1990) 127.
15. B. JIMENEZ, C. ALEMANY, J. MENDIOLA and E. MAURER, *J. Phys. Chem. Solids* **46** (1985) 1383.
16. T. TSURUMI and Y. HOSHINO, *J. Amer. Ceram. Soc.* **72** (1989) 278.
17. S. B. DESHPANDE, H. S. POTDAR, P. D. GODBOLE and S. K. DATE, *ibid.* **75** (1992) 2581.
18. H.-Y. LEE and R. FREER, *J. Appl. Phys.* **81** (1997) 376.
19. S. PEJOVNIK, D. KOLAR, W. J. HUPPMANN and G. PETZOW, in: "Sintering – New Developments", edited by M. M. Ristic (Elsevier Scientific, Amsterdam, 1979) pp. 285–92.

*Received 6 November
and accepted 5 December 1997*